04,05,10

Magnetic properties of bicomponent nanoparticles $CuO-CuFe_2O_4$, obtained by arc evaporation method

© M.P. Volkov[1], M.A. Yagovkina[1], V.P. Sedov[2], N.A. Lisaevich[2], D.S. Zdeshnev[1,3]

[1] Ioffe Institute,
St. Petersburg, Russia
[2] B.P. Konstantinov Petersburg Nuclear Physics Institute of National Research Center „Kurchatov Institute“,
Gatchina, Russia
[3] Peter the Great Saint-Petersburg Polytechnic University,
St. Petersburg, Russia

E-mail: m.volkov@mail.ioffe.ru

Received July 11, 2024
Revised July 16, 2024
Accepted July 17, 2024

Bicomponent $CuO-CuFe_2O_4$ nanoparticles with a $CuFe_2O_4$ content of about 20% were obtained using the arc evaporation method. X-ray examination showed that the samples contained only CuO nanoparticles with a size of 54 nm and $CuFe_2O_4$ with a size of 32 nm. The temperature dependences of the magnetization of nanoparticles $M(T)$ have a form characteristic of a superparamagnetic state with a blocking temperature above 400 K at $H = 100$ Oe. The field dependences of the magnetization $M(H)$ show high values of saturation magnetization at all temperatures studied. In low fields, the $M(H)$ dependences have a hysteretic character, and at low temperatures the loop has features associated with different contributions to the magnetization from the central part of the bicomponent particle ($CuFe_2O_4$) and from the peripheral part adjacent to CuO. The synthesis method using an arc discharge makes it possible to effectively obtain bicomponent particles that are similar in size and with high magnetization values up to a temperature of 400 K.

Keywords: bicomponent nanoparticles, arc evaporation, magnetization, hysteresis loop, superparamagnetism.

DOI: 10.61011/PSS.2024.09.59218.190

1. Introduction

Bicomponent nanoparticle, i. e. nanoparticles, each comprising two phases simultaneously, are currently the object of increased interest of researchers. Main reason of interest to bicomponent nanoparticles is that their physical and chemical properties can significantly differ from properties of initial components, and determined not only by small size of particles, but also by simultaneous occurrence of properties o both phases and by presence of interface between phases. The bicomponent nanoparticles formation is observed only for some compounds; in particular, such bicomponent nanoparticles are formed in system $CuO-CuFe_2O_4$. Attention of the researches to nanoparticles of this system is associated with possible use in medicine and engineering. In medicine use of nanoparticles $CuO-CuFe_2O_4$ to create antibacterial agents is based on that in such bicomponent particle CuO has antobacterial properties, and $CuFe_2O_4$ has strong magnetic properties and can be used as magnetic carrier. The bicomponent nanoparticles $CuO-CuFe_2O_4$ exhibit photocatalytic activity, which is associated with the presence of interface between the phases, due to which the recombination of photoinduced electron-hole pairs is reduced. Thus, in paper [1] degradation of methylene blue dye on surface of nanoparticles under sun light was studied, and it was identified that the efficiency of dye decomposition is by three times higher when using bicomponent nanoparticles $CuO-CuFe_2O_4$, than for nanoparticles $CuFe_2O_4$. The bicomponent nanoparticles $CuO-CuFe_2O_4$ are considered also as promising materials for creation of very sensitive gas detectors H_2S [2] and CO_2 [3]. Due to this study of bicomponent nanoparticles $CuO-CuFe_2O_4$ properties, in particular, of magnetic properties in wide range of magnetic fields and temperatures, is important objective in way of these particles use in medicine and engineering.

The compound CuO is low-dimensional antiferromagnetics with the Néel temperature $T_N = 230$ K. For CuO nanoparticles superparamagnetic behavior with weak ferromagnetism at low temperatures was detected [4]. At that in later papers it is shown that magnetic properties of CuO nanoparticle can significantly depend on size of particles. The nanoparticle with size about 10 nm demonstrate magnetization up to 0.1 emu/g in field 100 Oe at low temperatures [5]. For nanoparticles of copper ferrite $CuFe_2O_4$ superparamagnetic behavior with significantly larger magnetization is also observed — at room temperature the saturation magnetization reaches 50 emu/g for particles with size 40 nm [6] and 86 emu/g for particles with size 195 nm [1].

Magnetic properties of bicomponent nanoparticles $CuO-CuFe_2O_4$ were studied in some papers [1,7–10]. It was found that the bicomponent nanoparticles of this system could be prepared by different methods, at that

Methods of obtaining, dimensions and magnetic properties of bicomponent nanoparticles $CuO-CuFe_2O_4$ as per published data

Method of obtaining	D, nm	M_s (300 K), emu/g	M_r, emu/g	H_c, Oe	Studied property	Publications
Oxalate precursors and calcination of deposits	60	9.8 (at 20% Fe)	2.2	79	Optic. spectra in UV and visible range	[7]
Microemulsions in ethanolanol, calcination of deposits	54	7.44 (at 20% Fe)	3.8	1095	Optic. spectra in UV and visible range	[8]
Co-precipitation of nitrates in water and calcination of sediments	59.6 (D_{CFO})	4	1.8	1000	Dependence of parameters of loop $M(H)$ on cycling	[9]
Hydrothermal method with use of surfactants	36 (D_{CFO})	2.5	0.4	54	Photocatalytic properties during degradation of dyes	[10]
Ultrasound study of ferrum and copper chlorides in solution of ammonia and ethyleneglycol	40–300	72.6	~ 5	~ 100	Catalytic properties during degradation of dyes	[1]

all nanoparticles exhibiting superparamagnetic behavior with the blocking temperature increased with particle size increasing , and the saturation magnetization increases with iron content increasing.

Table shows methods for nanoparticles obtaining, size of obtained particles D and their magnetic properties — saturation magnetization M_s, residual magnetizations M_r and coercivity field H_c at room temperature, and main physical and magnetic properties of obtained bicomponent nanoparticles studied in these papers.

It follows from the Table that magnetic properties of the obtained composite particles significantly depend on the method of obtaining. There is trend of saturation magnetization and residua; magnetization decreasing with decrease in size of nanoparticles. Maximum saturation magnetization $M_s = 72.6$ emu/g was reached for most coarse particles from 300 nm [1], which is little lower than $M_s = 86$ emu/g for rest nanoparticles $CuFe_2O_4$.

In present paper the magnetic properties were studied of bicomponent particles $CuO-CuFe_2O_4$, obtained by arc evaporation method.

2. Procedure of obtaining and study of properties of bicomponent nanoparticles

To obtain nanoparticles: $CuO-CuFe_2O_4$ copper-containing graphite electrode (a graphite tube whose cavity is filled with a mixture of copper compound with graphite powder) was evaporated in direct current electric arc (current 100–200 A, voltage 25–36 V) in helium atmosphere. The obtained carbon condensate in form of fine copper-containing soot was subjected to thermal oxidation in air. When using iron-containing tools and containers, the condensate (soot) also contains nanoparticles with high magnetization, which can be isolated by magnetic separation from non-magnetic carbon soot.

The phase composition of the obtained samples was studied by X-ray diffraction phase analysis (XDPA) on a D2 Phaser diffractometer (Bruker, Germany) (copper tube, wavelength $\lambda = 1.5406$ Å, accelerating current and voltage — 10 mA and 30 kV) equipped with a PSD-detector. The phase composition was interpreted using the Eva software package (Bruker) based on the ICDD database (PDF 2, release 2014).

To carry out magnetic measurements, the obtained powders were placed in a non-magnetic capsule, which was installed on the insert of the vibration magnetometer included in PPMS-14 unit.

Elementary analysis for iron content was performed using scanning-electron microscope „TESCAN VEGA 3 SBH“ (Czech Republic), by method of energy-dispersive spectroscopy. Data were processed using software „Aztec“ from „Oxford Instruments“.

Alternatively, the iron content in the test sample was determined using the chemical method of spectrophotometric analysis by the absorption of the ion complex Fe^{3+} with ammonium thiocyanate in a copper-containing solution.

3. Results and discussion

3.1. Structure and composition

The X-ray diffraction analysis showed (Figure 1), that powder comprises two phases only: CuO and $CuFe_2O_4$. Phase CuO (tenorite) has a monoclinic structure with lattice parameters $a = 4.69$ Å, $b = 3.42$ Å, $c = 5.13$ Å, $\beta = 99.48°$, and phase $CuFe_2O_4$ (cuprospinel) — cubic structure with the parameter $a = 8.36$ Å. Percentage content of phases in nanoparticles is 80% CuO and 20% $CuFe_2O_4$. The iron content in the sample weight, determined by

elemental analysis, was 6.6 wt%, and using the chemical method — 6.5 wt%.

By broadening of the diffraction peaks we can determine average size of coherent scattering region. For nanoparticles this region coincides size of individual phase of biorystal nanoparticles. Size of nanoparticles D for both phases was calculated by Scherrer formula:

$$D = \frac{K_\beta \lambda}{\beta \cos\theta},$$

where D — average size of crystallite, λ — wavelength of X-ray radiation, K_β — Scherrer constant (can be accepted equal to 1); θ — diffraction angle, β — reflex width at half maximum, average size of particles CuO is 54 nm and particles $CuFe_2O_4$ — 31 nm. Ratio of average volumes of particles of to phases (i.e. ratio of third degrees of average sizes) is about 1:5, this is close to ratio $20:80 = 1:4$, obtained by ratio of relative height of peaks of X-ray diffraction.

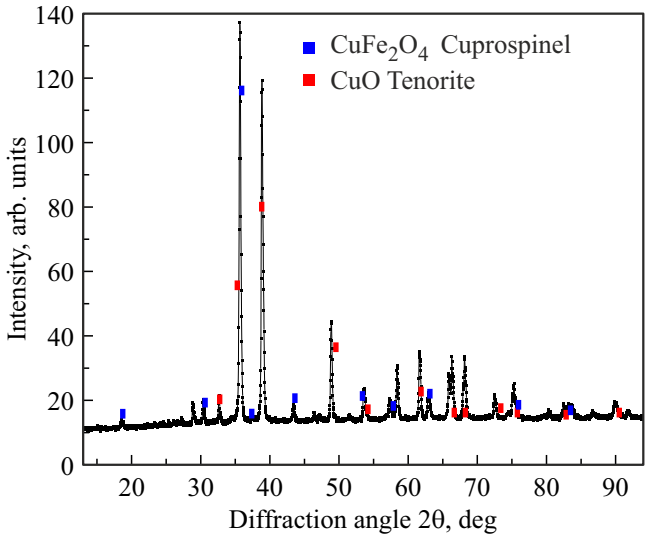

Figure 1. Spectra of X-ray diffraction for sample $CuO-CuFe_2O_4$; diffraction peaks for $CuFe_2O_4$ are marked with blue, with red — for CuO.

3.2. Magnetic properties

Figure 2 shows the temperature dependences of the specific magnetic moment of nanoparticles measured in FC (Field Cooling — cooling with field presence) and ZFC (Zero-Field Cooling — cooling without field and heating with field presence) modes at two values of the applied magnetic field: $H = 100$ and 1000 Oe.

For $H = 100$ Oe magnetic moment in ZFC mode with temperature rise quickly increases in temperature range 0–50 K, then magnetic moment rise rate decreases. When recording in FC mode the monotonous change in magnetic moment is observed. Note that 400 K is not blocking temperature (400 K — maximum temperature of unit): curves convergence will occur at higher temperatures. For $H = 1000$ Oe similar features are observed $M(T)$ in region 0–50 K in ZFC mode. ZFC and FC curves cross already at 60 K. Dependence $M(T)$ in FC mode also demonstrates monotonous increase in magnetic moment with temperature decreasing.

The type of dependences $M(T)$ in ZFC and FC modes is typical for nanoparticles in the superparamagnetic state: the curves diverge greatly in these modes, and with increase in the applied field the blocking temperature decreases. Relatively high value of specific magnetic moment is associated with magnetic properties of $CuFe_2O_4$ (almost 4 emu/g at low temperature and $H = 1$ kOe). In paper [9] close values of the specific magnetic moment (2 emu/g) is observed under same conditions (low temperatures and $H = 1$ kOe) for nanoparticles $CuO-CuFe_2O_4$ with same size of nanoparticles $CuFe_2O_4$ (31 nm).

The dependences $M(H)$ were measured at temperatures 2 and 300 K to $H = 1$ T and at temperatures 2, 10, 100, 200, 300 and 400 K — up to fields 0.1 T.

Figure 3 presents the dependence $M(H)$ for bicomponent nanoparticles $CuO-CuFe_2O_4$ at $T = 2$ and 300 K in fields

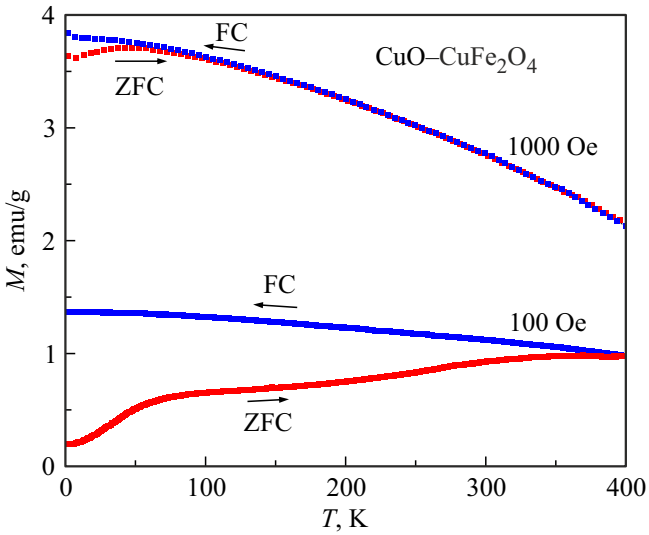

Figure 2. Dependences $M(T)$ for $H = 100$ and 1000 Oe in modes ZFC and FC.

below 10 kOe. It is evident that in low fields the hysteresis behavior of the ferromagnetic type is observed, and at fields above 2 kOe a saturation is observed at magnetization value of 3 emu/g at 300 K and 5 emu/g at 2 K. The magnetization decreasing with temperature rise corresponds to behavior of $CuFe_2O_4$, in which temperature of magnetic ordering is ~ 500 K. Figure 3 also presents dependence $M(H)$ at $T = 300$ K for nanoparticles $CuO-CuFe_2O_4$ with close dimensions $D_{CuFe_2O_4} = 36$ nm from paper [10].

In Figure 4 dependences $M(H)$ at $T = 2$ and 400 K are presented in region of magnetic fields up to 1000 Oe, where hysteresis behavior is observed. The presence of ferromagnetic hysteresis is visible even at high temperature

of 400 K, a significant expansion of the hysteresis at low temperature of 2 K and the appearance of features on the dependence $M(H)$ at low temperature. At $T = 2$ K there are kinks in dependence $M(H)$ in region of low fields and small asymmetry of hysteresis loop, this can be associated with two circumstances: 1) at low temperature the influence of the magnetic properties of CuO nanoparticles should be taken into account — thus, in paper [10] it was shown that CuO particles with average size of 27 nm have a hysteresis magnetization up to 0.1 emu/g at low temperatures; 2) at interface of CuO and $CuFe_2O_4$ effects of interaction of two magnetic structures can occur. The evidence of such interaction is presence of hysteresis loop asymmetry at

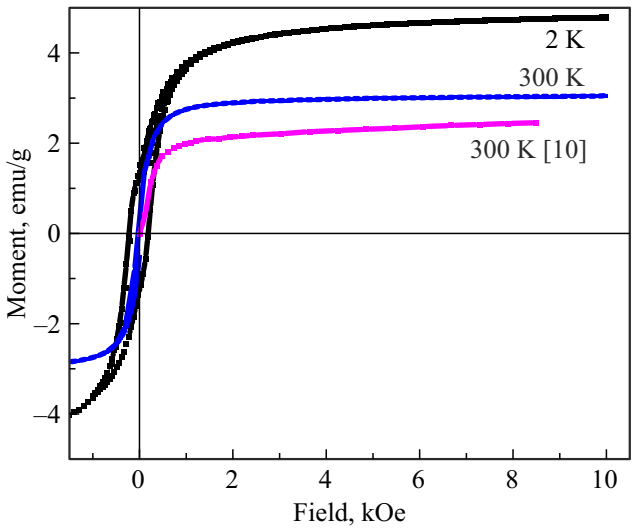

Figure 3. Dependence $M(H)$ for bicomponent nanoparticles $CuO-CuFe_2O_4$ with size $D_{CuFe_2O_4} = 31$ nm at $T = 2$ and 300 K in present study and $M(H)$ at $T = 300$ K for nanoparticles $CuO-CuFe_2O_4$ with size $D_{CuFe_2O_4} = 36$ nm from paper [10].

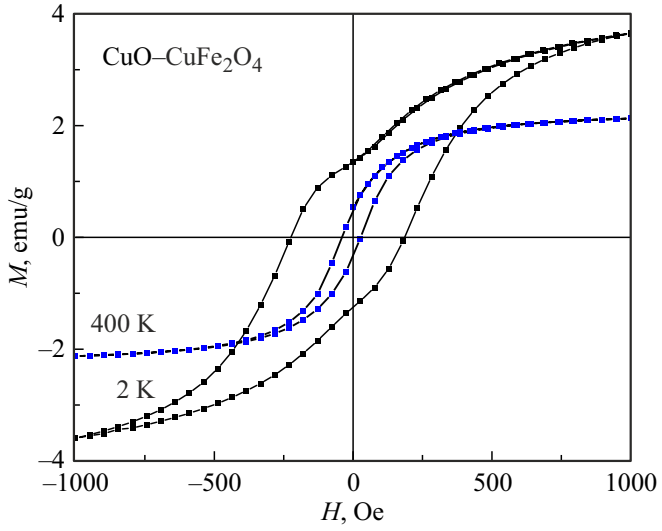

Figure 4. Dependence $M(H)$ for bicomponent nanoparticles $CuO-CuFe_2O_4$ at $T = 2$ and 400 K in magnetic field below 1000 Oe.

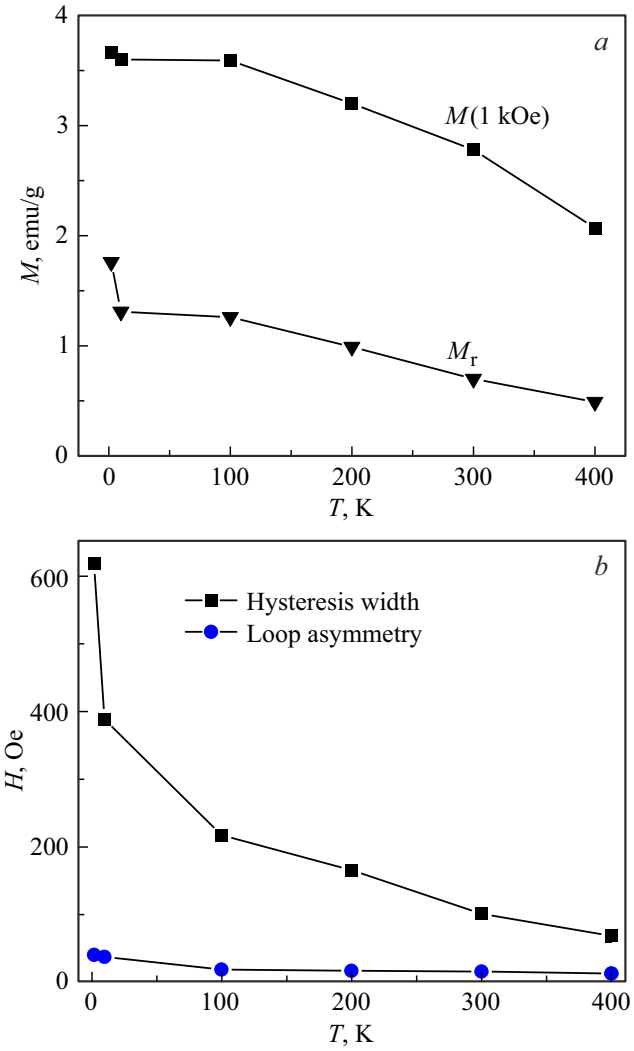

Figure 5. Temperature dependences *a* — values of saturation magnetization M (1 kOe) and residuael magnetization M_r and *b* — hysteresis loop width and values of loop asymmetry for sample $CuO-CuFe_2O_4$.

low temperature — effect of exchange offset. In studied bicomponent nanoparticles $CuO-CuFe_2O_4$ this effect is associated with interface of ferromagnetic phase $CuFe_2O_4$ and antiferromagnetic phase CuO, and was studied in detail in some papers [9,10]. Figure 5 presents temperature dependences of features of hysteresis loop: value of saturation magnetization M (1 kOe) and residual magnetization Mr (Figure 5, *a*), and width of hysteresis loop and value of loop asymmetry (Figure 5, *b*). All these values decrease with temperature increasing, but even at $T = 400$ K saturation magnetization and residual magnetization stay rather high — 2 and 0.5 emu/g, respectively.

4. Conclusion

By arc evaporation method nanoparticle $CuO-CuFe_2O_4$ with content of $CuFe_2O_4$ about 20% were obtained and

studied. The X-ray study showed that samples contain only nanoparticles CuO of size 54 nm and $CuFe_2O_4$ of size 32 nm.

The nanoparticle magnetization was measured in wide temperature range of 2 to 400 K. The temperature dependences $M(T)$, measured in FC and ZFC modes have form typical for supermagnetic state, and blocking temperature exceeds 400 K at $H = 100$ Oe; in field 1 kOe the blocking temperature decreases to 50 K. Measurements of field dependences of magnetization $M(H)$ showed that rather high values of saturation magnetization are observed during all studied temperatures and correspond to previously published results for 20% content of $CuFe_2O_4$. in low fields the dependences have hysteresis nature, loop width increases upon temperature decreasing and at 2 K reaches 500 Oe. At the lowest temperature the loop has features (kinks) that are associated with different contributions to the magnetization from the central part of bicomponent nanoparticle ($CuFe_2O_4$) and from periphery adjacent to CuO.

High values of magnetization indicate the efficiency of such nanoparticles use in cases, when magnetic control or magnetic separation is required, especially at temperatures exceeding 400 K.

Method of synthesis used during obtaining nanoparticles by arc discharge ensures effective production of bicomponent nanoparticles, close by size, with high values of magnetization up to temperature 400 K.

Conflict of interest

The authors declare that they have no conflict of interest.

References

[1] A. Massoud-Sharifi, G.K. Kara, M. Rabbani. Proceed. 4th Int. Electronic Conf. on Water Sci. **48**, *1*, 17 (2020).
[2] X. Hu, Z. Zhu, Z. Li, L. Xie, Y. Wu, L. Zheng. Sensors. Actuators B: Chemica **l264**, 139 (2018).
[3] T.P. Sumangala, Y. Thimont, V. Baco-Carles, L. Presmanes, C. Bonningue, I. Pasquet, P. Tailhades, A. Barnabé. J. Alloys Compd. **695**, 937 (2017).
[4] G. Narsinga Rao; Y.D. Yao, J.W. Chen. IEEE Trans. Magnetics **41**, *10*, 3409 (2005).
[5] A.A. Lepeshev, I.V. Karpov, A.V. Ushakov, D.A. Balaev, A.A. Krasikov, A.A. Dubrovskiy, D.A. Velikanov, M.I. Petrov. J. Supercond. Nov. Magn. **30**, *4*, 931 (2017).
[6] N. Masunga, O.K. Mmelesi, K.K. Kefeni, B.B. Mamba. J. Environ. Chem. Eng. **7**, *3*, 103179 (2019).
[7] M.M. Rashad, D.A. Rayan, A.A. Ramadan. J. Mater. Sci.: Mater. Electronics **24**, *8*, 2742 (2013).
[8] M.M. Rashad, S. Soltan, A.A. Ramadan, M.F. Bekheet, D.A. Rayan. Ceram. Int. **41**, *9 Part B*, 12237 (2015).
[9] Y.X. Gao, C.M. Zhu, S. Huang, Z.M. Tian, S.L. Yuan. J. Magn. Magn. Mater. **439**, 384 (2017).
[10] I.V. Karpov, A.V. Ushakov, V.G. Demin, E.A. Goncharova, A.A. Shaihadinov. JOM **72**, *11*, 3952 (2020).

Translated by I.Mazurov